Finite Element Simulation on Frictional and Brittle Preseismic fault slip

Zhishen Wu[(1)] Yun Gao[(1)] Yutaka Murakami[(2)]

(1) Department of Urban & Civil Engineering. Ibaraki University, Japan (e-mail: zswu@ipc.ibaraki.ac.jp; gaoyun@hcs.ibaraki.ac.jp, phone +81-294-38-5004 exe.5179 8077, Fax: +81-294-38-5268). (2) Geophysics Department, Geological Survey, Japan (e-mail: murakami@gsj.go.jp)

Abstract

In this paper, a finite element model for simulating crustal deformation including discontinuous slipping displacement along a fault is developed, where slip weakening behavior with a simple shear stress-relative displacement relationship on fault surface based on the concept of nonlinear fracture mechanics is taken into consideration. Throughout numerical simulations on fault-bend folding with a ramp, the contours and developments of the shear stress, the second stress invariant and the slip velocity varying with the values of fracture energy are investigated. Moreover, the breakdown process is discussed.

1 Introduction

It is known that many shallow earthquakes occur on plate boundaries and active geological faults, which are evidently pre-existing weakness in the shallow brittle part of the Earth. So far, numerous experimental studies on frictional sliding of pre-existing faults in rocks have been carried out for understanding mechanics of earthquake faulting.

From the initial rational knowledge, there are two basic laws of sliding friction: the frictional resistance is proportional to the normal load and it is independent of the apparent area of the sliding surfaces. Later, extensive and quantitative experimental investigations of friction have been performed by Amontons and Coulomb who have formulated the dry friction laws in the form which is still widely used and taught nowadays. In the frictional laws, the stress drop between static friction and dynamic friction is assumed to be constant. So the stress and slip velocity exhibit the singularity at that time. Although the frictional law is practically useful for estimating average source parameters of earthquakes, the singularity is physically unreasonable. To eliminate the stress singularity at the crack tip, Ida, Palmer and Rice developed a slip-weakening model. Then Andrews theoretically discussed the critical crack length for unstable rupture for 2D shear cracks. Since the slip velocity and the slip acceleration due to the cohesive force have finite values near the crack tip as theoretically shown by Ida, Ohnaka and Yamashita investigated the behavior of slip velocity and slip acceleration more in detail. Also, the slip-weakening behavior has been experimentally examined by many researchers from which it is found that quasi-stable sliding occurs on a localized region of a fault prior to unstable slip, the length of the localized region of quasi-stable sliding corresponds to the critical crack length for unstable rupture. But in general, present FEM method,

this effective model isn't considered. So in this paper, the finite slip-weakening model is introduced to a finite element method using a Lagrange description to avoid stress singularity.

2 Basic theory

In this present study, a structural system of fault-bend folding in which the reference configuration of a body exhibiting slipping along a fault surface so that the whole structural system is characterized by two constitutive relations. One is a volumetric constitutive law that relates stress and strain for body, while the other is a cohesive-softening and frictional surface constitute relation between the shear stress and relative displacement jumps for the fault. Using a Lagrange description, an attention is confined to quasi-static deformations and, with body forces, boundary forces and traction on internal fault surface considered, the incremental formulation of principle of virtual work is written as

$$\begin{aligned}\int_V \{de\}^T \{s + \Delta s\} dV &= \int_{S_0} \{du\}^T \{f_0 + \Delta f_0\} dS \\ &+ \int_{S_c} \{du\}^T \{f_c + \Delta f_c\} dS \\ &+ \int_V \{du\}^T \{r_0 + \Delta r_0\} dV\end{aligned} \tag{1}$$

The body is subjected to a body force field $\{r_0\}$ in V, prescribed external traction $\{f_0\}$ on force boundary S_0 and internal traction $\{f_c\}$ caused by relative displacement jump on discontinuous surface S_c. Here {s} is Lagrange stress vector; $\{e\}$ is Lagrange strain vector.

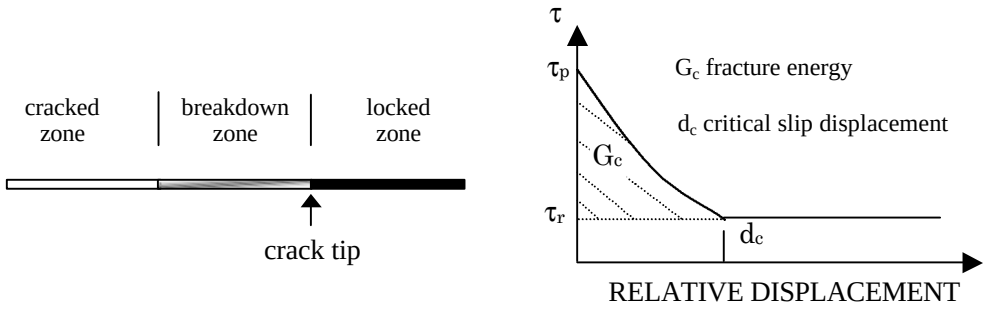

Fig.1 Three zones of different contact states between sliding surfaces on the fault and relation between shear stress and slip across a fault

To get the balance of the internal tractions on the two sides of the fault surface, master-slave method is used. For the constitute relation on the fault surface, the slip-weakening model shown in Fig.1 is adopted. The total fault surface of rocks can be consist of three zones: locked zone where sliding surfaces are strongly interlocked, breakdown zone where all the interlocked asperities are weakening until fractured and creaked zone which is behind the breakdown zone. The cohesive force between inner fracture surfaces is assumed to be a continuously decreasing function of relative displacement across the crack in order to eliminate the stress singularity at the crack tip. The relative displacement across the fault during the breakdown process is called the critical slip displacement d_c. The shaded area for the stress-slip relation is regarded as the energy required for creating new fracture surfaces of unit area or the work done by the cohesive force. This energy has been often called the fracture energy G_c, representing the rupture growth resistance.

Generally, in the locked zone, the incremental formulation of the fault traction can be obtained

through the incremental formulation of relative displacement $\{\Delta(\Delta u)\}$ and stiffness matrix $[K_c]$ on the fault surface

$$\{\Delta f_c\} = [K_c]\{\Delta(\Delta u)\} \tag{2}$$

$$t = f_t / lt \qquad s = f_n / lt \tag{3}$$

where τ and σ are the shear and normal stress on the fault surface; l is the length of interface element and t is the thickness. When the shear stress τ reaches to the value of peak stress τ_p which is equal to $\mu_s\sigma$, the weakening of the shear stress is beginning: μ_s is the static friction coefficient. Then the fracture energy begins to release. Thus, the incremental traction caused by relative displacement is added to the total incremental traction

$$\Delta f_t = K_t\left(\Delta(\Delta u_t) - \Delta u_c^w\right) \tag{4}$$

where Δu_c^w is the relative incremental weakening displacement which is the function of G_c, d_c, the tangent stiffness K_t and the relative displacement Δd from the beginning of initial weakening

$$\Delta u_c^w = \left(1 + \frac{2G_c lt}{K_t d_c^2}\right)\Delta d \tag{5}$$

As the fracture energy releases completely, the residual stress becomes to dynamic frictional stress which is assumed to obey the rate- and state-dependent friction law proposed by Ruina

$$\begin{aligned} t_r &= m_d\, s \\ m_d &= m_0 + q + a\ln(V / V_*) \\ \frac{dq}{dt} &= -\frac{V}{L}[q + b\ln(V / V_*)] \end{aligned} \tag{6}$$

where μ_d is the dynamic friction coefficient , V is sliding velocity of an element and V_* is a reference velocity given arbitrarily. The constants μ_0, a, b and L characterize the frictional property. Generally, $dq / dt = 0$ means steady-state.

3 Numerical simulation

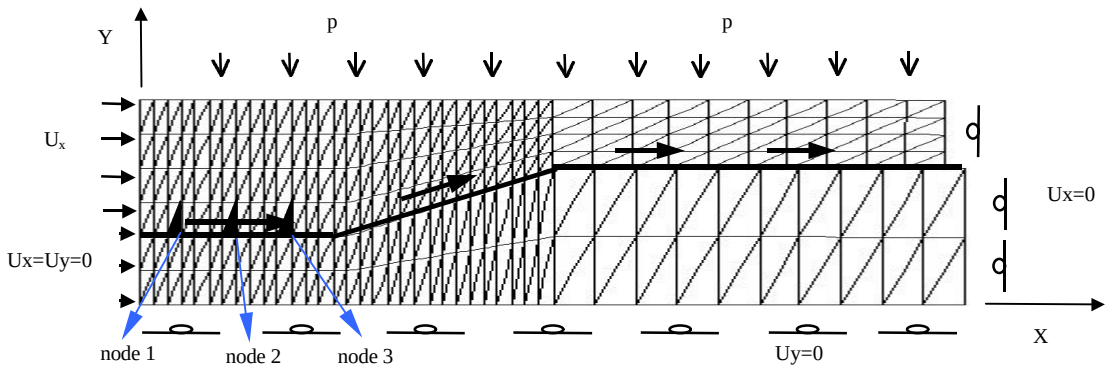

Fig.2 Initial, undeformed grid for the finite-element model, showing boundary conditions

Fig.2 shows a finite element mesh of a structural model with fault-bend folds, whose responses in long time have been investigated very well. In this paper, we focus on the effect of the response in short time and weakening material behaviors on the fault surface. Each structural model contains 480 6-node isoparametric, quadratic triangle elements. Plane strain is assumed. The initial fault geometry consists of a 2000m long and 500m high ramp connecting lower and upper flats. A surface pressure of 75 MPa is applied to the top of the hanging wall, which simulates a 3km overburden. There is zero shear stress along this top surface of the model. A zero displacement boundary

condition, $U_x=U_y=0$, is used along the left (hinterland) side of the hanging wall and the footwall, $U_y=0$ along the base of the model and $U_x=0$ along the right (foreland) side of the footwall. A displacement of 50cm per 50 year time step is imposed on the left side of the hanging wall, the velocity (1 cm y^{-1}) that is consistent with estimates of natural thrust sheet motion but the time step can automatic vary with different periods and different conditions. The shaded elements from left to right are named as element 1,2 and 3. Moreover, the below-right corner-node of element 1 is named as node 1 and by the same method, node 2,3 are named.

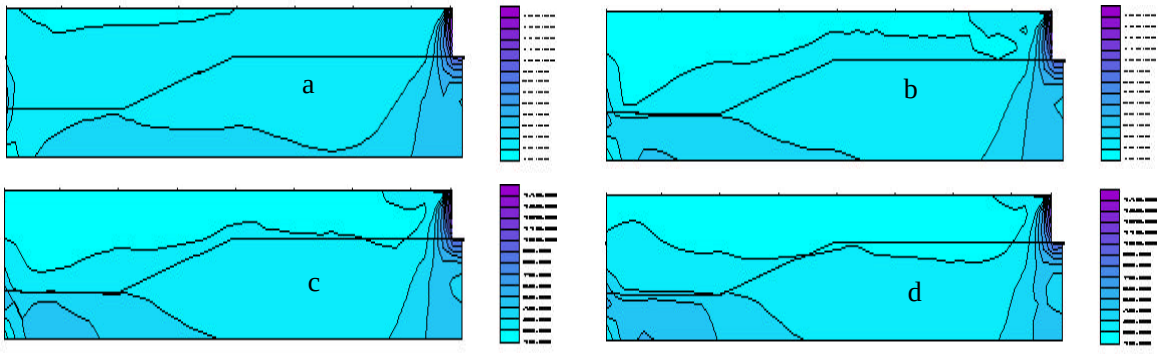

Fig.3 Contours of $(J_2)^{1/2}$ (a)in initial time (b) in weakening of node 1 (c) in weakening of node 2 (d) in weakening of node 3

Fig.3 shows the contours of $(J_2)^{1/2}$ in different period as $\mu_s=0.25$, $\mu_d=0.20$, $K_t=1.2\times10^7$ Pa and $G_c=1\times10^5$ Jm^{-2}, where it is 10MPa per layer of right bar. It is found that at every time, the higher values accumulate in the right side of the forelands of the hanging wall and footwall. Collating the initial contour, at the time when the node 1 is weakening, in the hanging wall, the area of low value enlarges from the hinterland to the foreland; and also, in the footwall, the area with higher J_2 in the hinterland enlarges. When the node 2 is weakening, collating Fig.3b, in the hanging wall, the area of low value enlarges to the foreland but reduces from the hinterland; and the area with higher J_2 in the hinterland enlarges continuously. Contrasting with Fig.3c, when the node 3 is weakening, in the hanging wall, the area of low value also enlarges to the foreland and also reduces from the hinterland; and the area with higher J_2 in the hinterland also enlarges continuously. Furthermore, by the total trend, the nodes on the fault surface are yielding from left to right, but in some local areas specially, some right nodes are yielding even earlier than their near left nodes.

By following two individual particles as shown in Fig.2, the stress paths in J space, shear stress and relative velocity can be tracked. From Fig.4a, node 1 begins to be weakening in the 270th year and node 3 begins in the 670th year. In the total period, though shear stresses has been weakened, the value of the $(J_2)^{1/2}$ trembles very small. Moreover, they become lower until some time and from this time, they begin to rise. For the relative velocity, the unsteady phenomenon can be observed. From Fig.4c, the value of the velocity is smaller of 5×10^{-9} m/s, and occasionally, the magnitudes exceed 1×10^{-8} m/s at some time. For most of the total period, it is steady slip. But at some time when there are some jumps or drops produced by the weakening of the shear stress, the unsteady slip occurs. From Fig.4d and Fig.4e, the biggest magnitude as $G_c=1\times10^3$ Jm^{-2} exceeds 2×10^{-4} m/s and the biggest magnitude as $G_c=0$ Jm^{-2} exceeds 2×10^{-3} m/s. Base on the same reason, the unsteady slips emerge, and with the decrease of the G_c, the unsteady slips increase. This unsteady phenomenon is as same as the results from rock experiments by which the slow earthquake and silent earthquake can be

simulated. From these experiments, when the stiffness of test machine is K, the dependence of frictional traction f and slip displacement u is described with |df/du|, if |df/du|<K, the slip is steady. On the contrary, the slip is unsteady. For the case of Fig.4c, the value of the |df/du| is always smaller than K in most of the period, so its unsteady slips are very few. On the other hand, for the case of Fig.4d and Fig.4e, the order that the value of the |df/du| is larger than K in most of the period increases, so the unsteady slip increases.

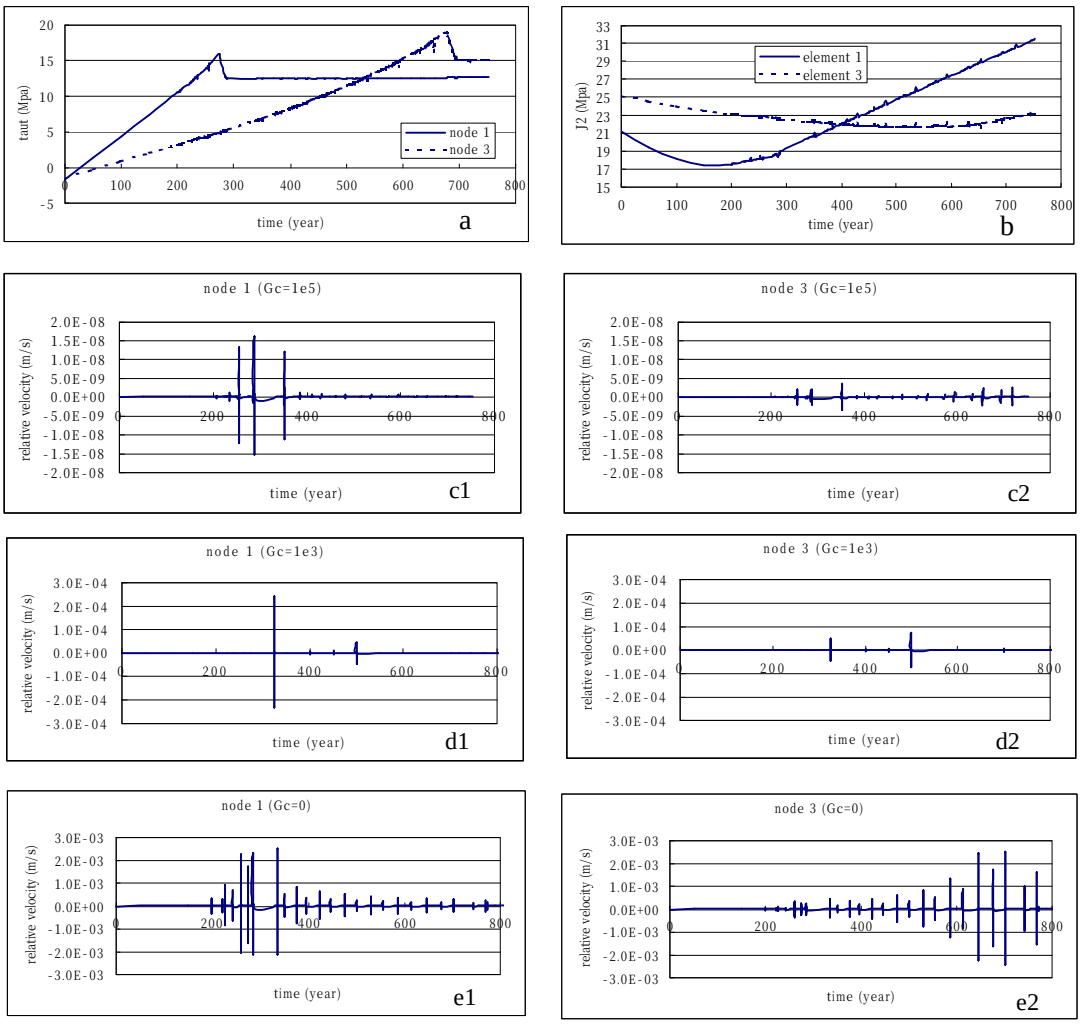

Fig.4 (a)shear stress (b) $(J_2)^{1/2}$ (c)relative velocity as $G_c=1\times10^5$ Jm^{-2} (d)relative velocity as $G_c=1\times10^3$ Jm^{-2} (e)relative velocity as Gc=0 with time for element 1 & 3 or node 1 & 3

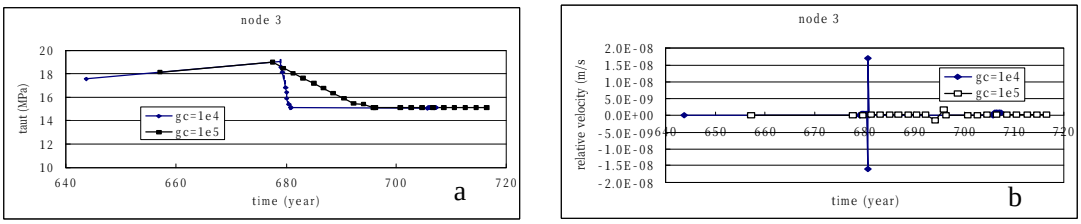

Fig.5 (a) shear stress of node 3 (b)relative velocity of node 3 as $G_c=1\times10^4$ Jm^{-2} and $G_c=1\times10^5$ Jm^{-2}

Fig.5a show the weakening processes of node 3 with different values of G_c. If the G_c is larger, the weakening time is longer and the magnitude of the relative velocity is smaller as shown in Fig.5b. Furthermore, the time beginning to weaken is same nearly. When the simulations are compared with different μ_d while the other material parameters are the same, the case with smaller μ_d will be weaken earlier with shorter weakening period as shown in Fig.6. Even though its magnitude of relative velocity is larger, the magnitude order is same. When the simulations are compared with different K_t, it is found that the case with larger K_t will be weaken earlier with shorter weakening period but its magnitude order of the magnitude of relative velocity is larger as shown in Fig.7.

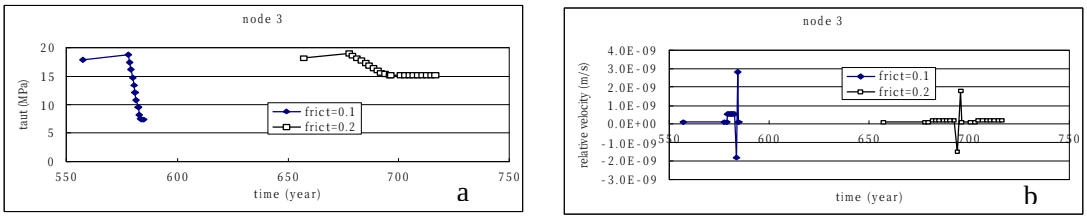

Fig.6 (a) shear stress of node 3 (b)relative velocity of node 3
as μ_d=0.1, 0.2 and μ_s=0.25

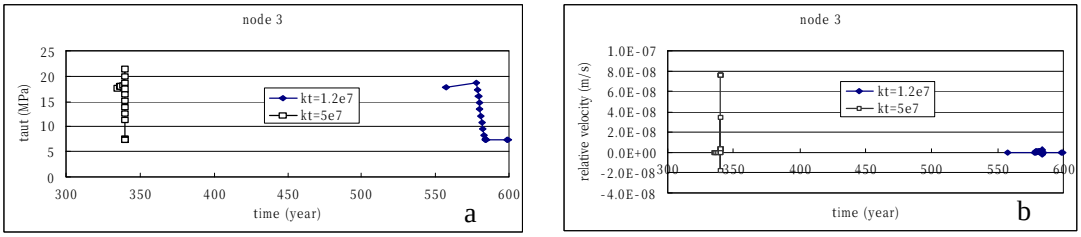

Fig.7 (a) shear stress of node 3 (b)relative velocity of node 3
as $K_t=1.2\times10^7$ MPa and $K_t=5.0\times10^7$ MPa

4 Conclusions

From the above numerical simulations, it can be concluded that:

(1) There are unsteady slips as G_c=0, 1×10^3 and 1×10^5 Jm^{-2}, but with the decrease of the G_c, the unsteady slips increase.

(2) When the weakening of the shear stress appears, the second invariant varies hardly, however, the variety of the relative velocity is huge.

(3) When the K_t increases, or the μ_d decreases, or the G_c decreases, remarkably, the magnitude of the relative velocity increases obviously. Moreover, the start time of the weakening process is also effected by the material parameters K_t and μ_d.

Reference

1) Erickson & Jamison: Viscous-plastic finite-element models of fault-bend folds, Jour. Stru. Geol, Vol 17, No.4, 561-573, 1995

2) Zhishen Wu, Yun Gao & Yutaka Murakami: A finite element model for crustal deformation with large slipping on fault surface, International workshop on solid earth simulation and ACES WG meeting, 2000

3) Yun Gao, Zhishen Wu & Yutaka Murakami: Viscous-plastic analysis of crustal deformation of fault-bend folds, Jour. Appl. Mech., Vol.3, 585-594,2000